J. Comp. Int. Sci. (2017) 8(2):53-68
http://epacis.net/jcis/PDF_JCIS/JCIS-0122.pdf
jcis@epacis.net

Pan-american Associacion of Computational Interdisciplinary Sciences

Simulation of fluid dynamics and CO_2 gas exchange in the alveolar sacs of the human lung

Luis J. Caucha [a1], Obidio Rubio [b], Alexis Rodrigues Carranza [b]

[a] Universidad Nacional de Tumbes, Perú
[b] Universidad Nacional de Trujillo, Perú

Received on November 25, 2016 / Accepted on May 30, 2017

Abstract

We present a mathematical model describing the dynamics of CO_2 gas transport in the alveolar sacs of the human lung, during the mechanism of inspiration and expiration that includes the gases exchange with the cardiovascular system. To deal with the domain movement, we use Arbitrary Lagrangian Eulerian (ALE) framework and equal-order finite elements in combination with pressure-stabilization techniques based on local projections. The model shows that the energy dissipation depends on geometrical deformation of alveolar sac and physical properties of the fluid.

Keywords: Gas dynamic, ALE, Alveolar Sac, FEM.

1. Introduction

We are interested in a model for describing the dynamics of carbon dioxide (CO_2) gas transport in the alveolar sac of the human lung. The gas transport in the lung was studied using one-dimensional mathematical model proposed by Scherer et al. [1], showing the stratification of gas for each respiration in the 24 generations of the lung, this model used a trumpet anatomical model of the lung proposed by Weibel [2], those generations represents a bifurcation of the bronchial tree, starting from trachea (0th) to terminal bronchioles (23rd); the alveolus appeared from 16th generation to 23rd, in this zone the gases exchange take place and the wall deformation is produced as a consequence of inspiration and expiration mechanism.
Considering the ideal gas conditions in the alveolus, such as instantaneous homogeneity for the gas in a respiration, Engel and Paiva [4, 3] developed a mathematical model [6, 5]. After that, Swan et al. [7], and Federspiel et al. [8], analyzed the dispersion in the alveolar ducts, using the Navier-Stokes equation and convection-diffusion equation for the gas transport; that research was made on the rigid domain, but during the respiration of alveolar

[1]E-mail Corresponding Author:ljcaucham@untumbes.edu.pe

doi: 10.6062/jcis.2017.08.02.0122

sacs is moved according to inspiration or expiration process.
In this article, we considered a moving domain for the simulation of the gas exchange and transport in the alveolar sac, especially the CO_2 alveolar distribution. The principal assumptions considered for this analysis were the gas exchange in the alveolar zone, because it is a principal source of CO_2 from blood circulation to alveolar; the fluid flow in the alveolar sac is governed by the incompressible Navier-Stoke equation and the transport equation for the CO_2 gas, those equations on the moving domain were transformed to the Arbitrary Lagrangian-Eulerian coordinate [10, 9, 11], such that by a map the moving domain was defined in a fixed domain.
The simulation for the changes in the inspiration and expiration condition, we used the Neumann and Dirichlet condition respectively, and using Nitsche's method those conditions were incorporated in the variation formulation. For discretization, we use equal-order finite elements in combination with a pressure stabilization technique, *Local Projection Stabilization* (LPS) method [12], the code was implemented in Gascoigne3D [13]. The article was structured by: the section 2, we showed the equations for the fluid and gas transport, with their initial and boundary conditions. In Section 3, we transformed the weak system equations of the Eulerian coordinate to Arbitrary Lagrangian-Eulerian coordinates, furthermore an analysis of weak solution in ALE coordinate of the system equation. In section 4, we introduce a finite element discretization and describe the pressure stabilization techniques, especially on moving domains. We present numerical results in Section 5, where we study alveolar sacs in the distal zones. Finally, we conclude in Section 6.

2. Mathematical model

The respiration consist in inhale and exhaled of air, in some research the room air could be replace by a mix of tracer gases as example Argon (Ar), Helium (He) and Sulfur Hexafluoride (SF6) or pure oxygen [15, 14, 16]. In this model we consider room air, the fluid transports gases such as oxygen (O_2) and carbon dioxide (CO_2); each gas is governed by a transport equation with the physic characteristics, the system equations is described by:

2.1. Equation for the fluid flow

The assumptions considered for the analysis of the fluid is that partial pressure outside (room air) and inside of the lung is practically constant (for example the Nitrogen), and moreover the temperature in the lung is

constant, it follow us considered as an incompressible fluid as:

$$\begin{cases} \rho\partial_t u + \rho(u\cdot\nabla)u - div\sigma = 0 & , \ in\ \Omega(t), \\ div(u) = 0 & , \ in\ \Omega(t), \\ u = V^{dom} & , \ in\ \Gamma_{bl}\cup\Gamma_w, \\ \sigma\eta = 0 & , \ in\ \Gamma_{io}, \end{cases} \tag{1}$$

where: $\Omega(t)$ is the domain representing the alveolar sac geometry, this domain changes as a function of time, V^{dom} (velocity of moving domain).
The boundary has three different parts such that: Γ_{bl} is the part for gas exchange between alveolar gas and the blood flow; Γ_w is the wall there is not exchange and Γ_{io} is the boundary where the inflow and outflow take place as a consequence of inhalation and exhalation.(see figure 1)

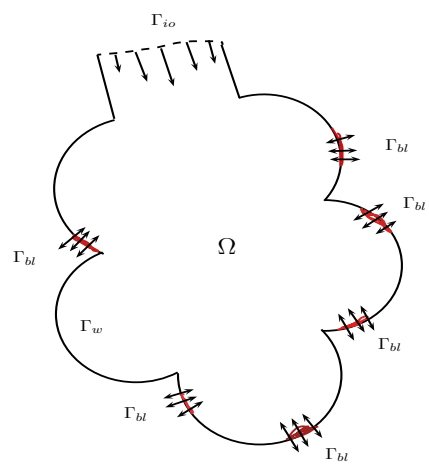

Figure 1 - Geometry of alveolar sac.

For the incompressible fluid, the Cauchy tensor was

$$\sigma = \rho\nu\nabla u - pI; \tag{2}$$

This is used in the system 1, where ρ is the fluid density, u velocity and p pressure.
In the model, we considered outside of the alveolar sac as approximate value Caucha et al. [17] and the boundary Γ_{io} such that do-nothing condition [18]. We considered the *inflow* and *outflow* velocity is known for Γ_{io} (by experiment), such that the moving domain was considered as a variable.

2.2. Transport equation

As the CO_2 is moved from Γ_{bl} to Γ_{io}, we consider the convection-diffusion equation to simulated the transport of this gas, such that:

$$\begin{cases} \partial_t C + u \cdot \nabla C - D\Delta C = 0 & , \ in\ \Omega(t) \\ \partial_\eta C - \alpha_b(C_b - C) = 0 & , \ in\ \Gamma_{bl} \\ \partial_\eta C = 0 & , \ in\ \Gamma_w. \end{cases} \tag{3}$$

In the boundary Γ_{io}, we have the conditions for inflow and outflow CO_2 gas concentration such as:

$$\begin{cases} C = C_{\text{ext}} & , \ if\ v \cdot \eta < 0 \\ \partial_\eta C = 0 & , \ if\ v \cdot \eta > 0 \end{cases} \quad in\ \Gamma_{io}, \tag{4}$$

where, C is the CO_2 gas concentration in the alveolar sac, C_{ext} is the boundary condition Γ_{io} for inhalation, C_b gas concentration in the pulmonary blood flow and u fluid velocity, α_b constant of the gas solubility in the blood.
The Dirichlet condition (inhalation) and Neumann condition (exhalation) in the boundary Γ_{io} were include weakly in the variation formulation using Nitsche's method [19] such that:

$$\partial_\eta C - \gamma h^{-2}\mathcal{H}(v \cdot \eta)(C_{\text{ext}} - C) = 0,\ in\ \Gamma_{io}, \tag{5}$$

where γ is a parameter (dimensionless), moreover $h \to 0$ and $\mathcal{H}$ is the unit step function

$$\mathcal{H}(x) = \begin{cases} 1 & , \ x > 0 \\ 0 & , \ x \leq 0. \end{cases} \tag{6}$$

The initial condition for the velocity and concentration were $u(.,0) = v_o$, and $C(.,0) = C_o$.

3. Weak formulation of the system equations

Considering the equation system for the fluid flow (1) and multiplied by a vectorial test function $\phi \in \left(C_0^\infty(0,t;\Omega)\right)^2$, and a scalar test function $\psi \in C_0^\infty(0,t;\Omega)$; then integrating in $\Omega(t)$; such that the equation is weakened in the sense of distributions; We have the weak variational formulation of the model for the dynamic of fluid and CO_2 gas transport in Eulerian coordinate as :
Find $u \in V^{dom} + \mathcal{V}, p \in \mathcal{L}, C \in \mathcal{H}$ such that

$$\begin{cases} (\rho\partial_t u + \rho(u\cdot\nabla)u, \phi) + (\sigma, \nabla\phi) = 0, & \forall\phi \in \mathcal{V} \\ (\mathrm{div} u, \xi) = 0, & \forall\xi \in \mathcal{L} \\ (\partial_t C + u\cdot\nabla C, \psi) + (D\nabla C, \nabla\psi) - (\alpha(C_b - C), \psi)_{\Gamma_{bl}} - & \\ (\gamma h^{-2}\mathcal{H}(u\cdot\eta)(C_{\text{ext}} - C), \psi)_{\Gamma_{io}} = 0 & ,\forall\psi \in \mathcal{H}. \end{cases} \tag{7}$$

Where $\mathcal{V} = \left(\overline{C_0^\infty(\Omega(t); \partial\Omega\backslash_{\Gamma_{bl}\cup\Gamma_w}}^{\|.\|_{H_0^1}}\right)^2$, $\mathcal{L} = \overline{C_0^\infty(\Omega(t))}^{\|.\|_{L^2}}$, $\mathcal{H} = \overline{C_0^\infty(\Omega(t))}^{\|.\|_{H^1}}$, and the initial conditions $u(.,0) = u_o$, $C(.,0) = C_o$.

3.1. Arbitrary Lagrangian-Eulerian (ALE) method for moving domain

In order to observe the effect of movement of domain in the fluid dynamic, we introduced a reference domain fixed $\hat{\Omega} \subset \mathbb{R}^2$, and the map $\hat{T}(t)\colon \hat{\Omega}_o \to \Omega(t)$.

Utilizing this map to transform the equations system (1) to reference domain and define velocity, pressure and gas concentration in the reference system, such variables of interest are

$$\hat{v}(\hat{x}, t) = v(\hat{T}(\hat{x}, t), t), \;\; \hat{p}(\hat{x}, t) = p(\hat{T}(\hat{x}, t), t), \;\; \forall\hat{x} \in \hat{\Omega}_o.$$

Considering the map $\hat{T}$ a C^1-diffeomorphism ; we transform the system equation on $\hat{\Omega}_o$ using $\hat{v}$, $\hat{\rho}$ and $\hat{C}$ as principal variables. This method is called Arbitrary Lagrangian- Eulerian [20], such that it allow made an analysis Eulerian- Lagrangian in a fixed domain; this is an advantage for the numerical approximation.

Considering $\Omega(t)$ as the domain that represent the Eulerian movement of the fluid as a consequence of inflation and deflation of the alveolar sac by the respiratory cycle, and $\hat{\Omega}_o$ the reference system that represent the rest, it is dependent of the respiratory cycle started could be Functional Residual Capacity (FRC) or Residual Volume (RV) of the lung. Furthermore, we add an arbitrary fixed domain $\hat{W}$ such that $\hat{\Omega}_o = \hat{W}$ without considering some physical meaning. Considering $\hat{W}$ fixed in the time, there is exist an invertible map $\hat{T}_w(t)\colon \hat{W} \to \Omega(t)$ with gradient $\hat{F}_w := \nabla\hat{T}_w$ and Jacobian $\hat{J}_w = \det(\hat{F}_w)$, which F_w and J_w have the properties of deformation of Lagrangian gradient , the Lagrangian particle $\hat{x} \in \hat{\Omega}_0$, the Eulerian path $x(\hat{x}, t) \in \Omega(t)$ and $\hat{x}_w \in \hat{W}$ with $\hat{T}_w(\hat{x}_w, t) = x = \hat{T}(\hat{x}, t)$; we must consider the difference between the velocity $\partial_t\hat{T}_w$ (velocity of movement of the reference system) and the physic velocity $\hat{V}$ [23, 21, 22].

Transformed the systems equation (1) to ALE coordinate, such that the variables of interest are $\hat{v}$, $\hat{p}$ and $\hat{C}$, we have:

Find $\hat{v} \in \hat{\mathcal{V}}(\hat{\Omega})$, $\hat{p} \in \hat{\mathcal{L}}(\hat{\Omega})$ and $\hat{C} \in \mathcal{H}$ such that

$$\begin{cases} \rho(\hat{J}(\partial_t \hat{v} + \hat{F}^{-1}(\hat{v} - \partial_t \hat{T}) \cdot \hat{\nabla})\hat{v}, \hat{\phi})_{\hat{\Omega}} + (\hat{J}\hat{\sigma}\hat{F}^{-T}, \hat{\nabla}\hat{\phi})_{\hat{\Omega}} & = 0, \ \ \forall \hat{\phi} \in \hat{\mathcal{V}} \\ (\hat{\mathrm{div}}(\hat{J}\hat{F}^{-1}\hat{v}), \hat{\xi})_{\hat{\Omega}} & = 0, \ \ \forall \hat{\xi} \in \hat{\mathcal{L}} \\ \big(\hat{J}(\partial_t \hat{C} + (\hat{F}^{-1}(\hat{v} - \partial_t \hat{T}) \cdot \hat{\nabla})\hat{C}), \hat{\psi}\big) + \big(D\hat{J}\hat{F}^{-T}\hat{\nabla}\hat{C}, \hat{\nabla}\hat{\psi}\big) - & \\ \big(\alpha(c_b - \hat{C}), \hat{\psi}\big)_{\hat{\Gamma}_{bl}} + \big(\gamma h^{-2}\mathcal{H}(\hat{v} \cdot \eta)(c_{ext} - \hat{C}), \hat{\psi}\big)_{\Gamma_{io}} & = 0, \ \ \forall \hat{\psi} \in \hat{\mathcal{X}}, \end{cases} \tag{8}$$

where the domain $\hat{\Omega}$ is fixed and the test spaces are defined as

$$\hat{\mathcal{V}}_{\hat{\Omega}} := \big(\overline{C_0^\infty(\hat{\Omega}, \partial\hat{\Omega}\backslash_{\hat{\Gamma}_{bl} \cup \hat{\Gamma}_w})}^{\|\cdot\|_{H_0^1}}\big)^2, \quad \hat{\mathcal{L}}_{\hat{\Omega}} = \overline{C_0^\infty(\hat{\Omega})}^{\|\cdot\|_{L^2}}, \ \ \hat{\mathcal{X}} = \overline{C_0^\infty(\hat{\Omega})}^{\|\cdot\|_{H^1}}. \tag{9}$$

The Cauchy tensor in the reference domain is

$$\hat{\sigma} := -\hat{P}I + \rho\nu(\hat{\nabla}\hat{v}\hat{F}^{-1}). \tag{10}$$

3.2. Weak solution in ALE coordinates for the Fluid

Taking a Navier-Stokes equations in ALE coordinate (8), we have the definition 1.

Definition 1. *We say that $\hat{v}$ is a weak solution of the system (8), if satisfy the following formulation*

$$\rho(\hat{J}(\partial_t \hat{v} + (\hat{F}^{-1}(\hat{v} - \partial_t \hat{T}) \cdot \hat{\nabla})\hat{v}, \hat{\phi})_{\hat{\mathcal{L}}^2(\hat{\Omega})} + (\hat{J}\rho\nu(\hat{\nabla}\hat{v}\hat{F}^{-1}), \hat{\nabla}\hat{\phi})_{\hat{\mathcal{L}}^2(\hat{\Omega})} = 0, \quad \forall\, \hat{\phi} \in \hat{\mathcal{V}}$$

in sense of distribution in $(0, T)$; such that

$$\int_0^T \rho(\hat{J}(\partial_t \hat{v} + (\hat{F}^{-1}(\hat{v} - \partial_t \hat{T}) \cdot \hat{\nabla})\hat{v}, \hat{\phi})_{\hat{\mathcal{L}}^2} \psi \, dt + \int_0^T (\hat{J}\rho\nu(\hat{\nabla}\hat{v}\hat{F}^{-1}), \hat{\nabla}\hat{\phi})_{\hat{\mathcal{L}}^2} \psi \, dt = 0,$$
$$\forall\, \psi \in C_0^\infty(0, T; \mathbb{R}).$$

Utilizing the condition of the function of free divergence [24], the ALE system (8) is equivalent to

$$\rho(\hat{J}(\partial_t \hat{v} + (\hat{F}^{-1}(\hat{v} - \partial_t \hat{T}) \cdot \hat{\nabla})\hat{v}, \hat{\phi}) + (\hat{J}\rho\nu(\hat{\nabla}\hat{v}\hat{F}^{-1}), \hat{\nabla}\hat{\phi}) = 0, \quad \forall\, \hat{\phi} \in \hat{\mathcal{V}}. \tag{11}$$

3.2.1. Energy equation for the fluid

As $\mathcal{H}_0^1(\hat{\Omega}) \hookrightarrow \hat{\mathcal{L}}^2(\hat{\Omega})$ is dense and continuous, we considered a base of $\hat{\mathcal{L}}^2(\hat{\Omega})$ formed by elements of $\mathcal{H}_0^1(\hat{\Omega})$ and use the Galerkin's method. So,

given $\{\hat{w}_i\}_{i=1}^{\infty}$ bases of $\hat{\mathcal{L}}^2(\hat{\Omega})$, with $\hat{w}_i \in \mathcal{H}_0^1(\hat{\Omega})$. Considering the finite dimension subspace $\hat{\mathcal{V}}_m$ and the element as lineal combination of the elements w_i following

$$\hat{u}_m = \sum_{j=1}^{m} \alpha_j(t)\hat{w}_j \tag{12}$$

such that $\alpha_j(t)$ are the scalar function and depend of the time t.
Considering $\hat{\phi}_m = \hat{u}_m$ and replacing in the equation (11), then ordering terms we have the *energy equation* such that:

$$\frac{1}{2}\rho\hat{J}\partial_t(\hat{u}_m,\hat{u}_m)_{\hat{\mathcal{L}}^2}+(\hat{J}\rho\nu(\hat{\nabla}\hat{u}_m\hat{F}^{-1}),\hat{\nabla}\hat{u}_m)_{\hat{\mathcal{L}}^2}+\hat{J}\rho(\hat{F}^{-1}(\hat{u}_m-\partial_t\hat{T})\cdot\hat{\nabla})\hat{u}_m,\hat{u}_m) = 0, \tag{13}$$

it gives us a priori estimates for weak solution; using Stoke's theorem [25], and ordering terms (see details on Caucha et al.[26]), we have that

$$\frac{1}{2}\partial_t\|\hat{u}_m\|^2_{\hat{\mathcal{L}}^2(\hat{\Omega})}+\nu\|\hat{F}^{-1}\|_{L^\infty}|\hat{\nabla}\hat{u}_m\|^2_{\hat{\mathcal{L}}^2(\hat{\Omega})}+\frac{1}{2}\|\hat{F}^{-1}\|_{L^\infty}\int_{\hat{\Omega}}|\hat{u}_m|^2\mathrm{div}(\partial_t\hat{T})\,d\hat{x} \leq 0 \tag{14}$$

applying the Poincaré's inequality to the equation (14), we have that

$$\frac{1}{2}\partial_t\|\hat{u}_m\|^2_{\hat{\mathcal{L}}^2(\hat{\Omega})}+\lambda\nu\|\hat{F}^{-1}\|_{L^\infty}\|\hat{u}_m\|^2_{\hat{\mathcal{L}}^2(\hat{\Omega})}+\frac{1}{2}\|\hat{F}^{-1}\|_{L^\infty}\int_{\hat{\Omega}}|\hat{u}_m|^2\mathrm{div}(\partial_t\hat{T})\,d\hat{x} \leq 0 \tag{15}$$

furthermore $\hat{T}$ is a C^1-diffeomorphism , then energy equation is

$$\partial_t\|\hat{u}_m\|^2_{\hat{\mathcal{L}}^2(\hat{\Omega})} + (2\lambda\nu\|\hat{F}^{-1}\|_{L^\infty} + \|\hat{F}^{-1}\|_{L^\infty}\|\mathrm{div}(\partial_t\hat{T})\|_{\hat{\mathcal{L}}^\infty(\hat{\Omega})})\|\hat{u}_m\|^2_{\hat{\mathcal{L}}^2(\hat{\Omega})} \leq 0,$$

applying the Grönwall's lemma, we have that

$$\|\hat{u}_m\|^2_{\hat{\mathcal{L}}^2(\hat{\Omega})} \leq \|\hat{u}_m(0)\|^2_{\hat{\mathcal{L}}^2(\hat{\Omega})}exp\big(-\big(2\lambda\nu\|\hat{F}^{-1}\|_{L^\infty}+\|\hat{F}^{-1}\|_{L^\infty}\|\mathrm{div}(\partial_t\hat{T})\|_{\hat{\mathcal{L}}^\infty}\big)t\big). \tag{16}$$

From (16) follow the Galerkin approximation $\hat{u}_m$ exist globally in the time; that is $T_m = \infty$. Additionally, we observe that the dissipation of the initial energy is a function of the viscosity and domain deformation. Furthermore, we have that

$$\{u_m\} \quad \text{is bounded in} \quad \hat{\mathcal{L}}^\infty(0,T;\hat{\mathcal{L}}^2(\hat{\Omega})). \tag{17}$$

Integrating from 0 to T the equation (16), we have

$$\int_0^T \frac{1}{2}\partial_t \|\hat{u}_m\|^2_{\hat{\mathcal{L}}^2(\hat{\Omega})}\, ds + \int_0^T \nu \|\hat{F}^{-1}\|_{L^\infty} |\hat{\nabla}\hat{u}_m\|^2_{\hat{\mathcal{L}}^2(\hat{\Omega})}\, ds +$$
$$\int_0^T \big(\frac{1}{2}\|\hat{F}^{-1}\|_{L^\infty} \int_{\hat{\Omega}} |\hat{u}_m|^2 \mathrm{div}(\partial_t \hat{T})\, d\hat{x}\big)\, ds \leq 0$$
$$\frac{1}{2}\|\hat{u}_m\|^2_{\hat{\mathcal{L}}^2(\hat{\Omega})} - \frac{1}{2}\|\hat{u}_m(0)\|^2_{\hat{\mathcal{L}}^2(\hat{\Omega})} + \int_0^T \nu \|\hat{F}^{-1}\|_{L^\infty} |\hat{\nabla}\hat{u}_m\|^2_{\hat{\mathcal{L}}^2(\hat{\Omega})}\, ds +$$
$$\int_0^T \big(\frac{1}{2}\|\hat{F}^{-1}\|_{L^\infty} \int_{\hat{\Omega}} |\hat{u}_m|^2 \mathrm{div}(\partial_t \hat{T})\, d\hat{x}\big)\, ds \leq 0$$
$$\int_0^T \nu \|\hat{F}^{-1}\|_{L^\infty} |\hat{\nabla}\hat{u}_m\|^2_{\hat{\mathcal{L}}^2}\, ds + \int_0^T \big(\frac{1}{2}\|\hat{F}^{-1}\|_{L^\infty} \int_{\hat{\Omega}} |\hat{u}_m|^2 \mathrm{div}(\partial_t \hat{T})\, d\hat{x}\big)\, ds \leq \frac{1}{2}\|\hat{u}_m(0)\|^2_{\hat{\mathcal{L}}^2}$$
$$\int_0^T \nu \|\hat{F}^{-1}\|_{L^\infty} |\hat{\nabla}\hat{u}_m\|^2_{\hat{\mathcal{L}}^2}\, ds \leq \frac{1}{2}\|\hat{u}_m(0)\|^2_{\hat{\mathcal{L}}^2}$$

$$\int_0^T |\hat{\nabla}\hat{u}_m\|^2_{\hat{\mathcal{L}}^2(\hat{\Omega})}\, ds \leq \frac{1}{2\nu\|\hat{F}^{-1}\|_{L^\infty}} \|\hat{u}_m(0)\|^2_{\hat{\mathcal{L}}^2(\hat{\Omega})} \tag{18}$$

we have that

$$\{\hat{u}_m\} \quad \text{is bounded in} \quad \hat{\mathcal{L}}^2(0,T;H^1_0(\hat{\Omega})), \tag{19}$$

Now, from (17), (19), exist $\hat{u}$, such that $\hat{u}_m \overset{*}{\rightharpoonup} \hat{u}$ in $\hat{\mathcal{L}}^\infty(0,T;\hat{\mathcal{L}}^2(\hat{\Omega})$ and $\hat{u}_m \rightharpoonup u$ in $\hat{\mathcal{L}}^2(0,T;\mathcal{H}^1_0(\hat{\Omega}))$, respectively.

3.3. Weak solution in ALE coordinates for the gas transport

For the system (8), we made an analysis of existence and uniqueness of the weak solution for gas concentration in the same way that for velocity.
For gas concentration $\hat{C}$. Utilizing the result for the velocity, those help us to make the estimates for transport equation.

Definition 2. *We say that $\hat{C}$ is a weak solution for the system (8) if it satisfy the next weak formulation*

$$(\hat{J}(\partial_t \hat{C} + (\hat{F}^{-1}(\hat{v} - \partial_t T)\cdot\hat{\nabla})C), \hat{\psi}) + (D\hat{J}\hat{F}^{-T}\hat{\nabla}\hat{C}, \hat{\nabla}\hat{\psi}) - (\alpha(c_b - \hat{C}), \hat{\psi})_{\Gamma_{bl}} +$$
$$(\rho h^{-2}\mathcal{H}(v\cdot\eta)(C_{ext} - \hat{C}), \hat{\psi}) = 0, \qquad \forall\, \hat{\psi} \in \hat{\mathcal{X}},$$

in the sense of distribution in $(0,T)$, such that

$$\int_0^T (\hat{J}(\partial_t \hat{C} + (\hat{F}^{-1}(\hat{v} - \partial_t T)\cdot\hat{\nabla})C), \hat{\psi})\phi\, dt + \int_0^T (D\hat{J}\hat{F}^{-T}\hat{\nabla}\hat{C}, \hat{\nabla}\hat{\psi})\phi\, dt -$$
$$\int_0^T (\alpha(c_b - \hat{C}), \hat{\psi})_{\Gamma_{bl}}\phi\, dt + \int_0^T (\rho h^{-2}\mathcal{H}(v\cdot\eta)(C_{ext} - \hat{C}), \hat{\psi})\phi\, dt = 0,$$
$$\forall\, \phi \in C_0^\infty(0,T;\mathbb{R}).$$

From the equation in the ALE coordinates, we have

$$(\hat{J}(\partial_t\hat{C} + (\hat{F}^{-1}(\hat{v} - \partial_t T)\cdot\hat{\nabla})C), \hat{\psi}) + (D\hat{J}\hat{F}^{-T}\hat{\nabla}\hat{C}, \hat{\nabla}\hat{\psi}) -$$
$$(\alpha(c_b - \hat{C}), \hat{\psi})_{\Gamma_{bl}} + (\rho h^{-2}\mathcal{H}(v\cdot\eta)(C_{ext} - \hat{C}), \hat{\psi}) = 0; \tag{20}$$

given the Faedo-Galerkin's approximation for the equation (20) with spaces $\mathcal{V}_m = span\{\hat{w}_1, \hat{w}_2, \cdots, \hat{w}_m\}$, $\hat{w}_i \in \mathcal{H}^1(\hat{\Omega})$ and $\mathcal{V}_m \subset \hat{\mathcal{L}}^2$, we have

$$\hat{C}_m = \sum_{j=1}^{m} \alpha_j(t)\hat{w}_j, \quad \hat{C}_m \in \mathcal{V}_m \tag{21}$$

where $\alpha_j(t)$ are a scalar function depending on the time. Replacing $\hat{C}$ by $\hat{C}_m$, taking $\hat{\psi}$ as an approximation in space $\mathcal{V}_m$.

3.3.1. Energy equation for the gas concentration

Replacing $\hat{\psi}$ by $\hat{C}_m$ in the equation (21), we have

$$\begin{aligned}&\hat{J}(\partial_t\hat{C}_m, \hat{C}_m) + (D\hat{J}\hat{F}^{-T}\hat{\nabla}\hat{C}_m, \hat{\nabla}\hat{C}_m) + \hat{J}(\hat{F}^{-1}(\hat{v} - \partial_t\hat{T})\cdot\hat{\nabla})\hat{C}_m, \hat{C}_m) - \\ &\langle\alpha_b(c_b - \hat{C}_m), \hat{C}_m\rangle_{\mathcal{H}^{-1/2}(\Gamma_{bl})} + \langle\gamma h^{-2}\mathcal{H}(C_{ext} - \hat{C}_m), \hat{C}_m\rangle_{\mathcal{H}^{-1/2}(\Gamma_{io})} = 0;\end{aligned} \tag{22}$$

with this equation, we be able to make the estimates a priori, those give us a weak solution defined in (2).
Using Stoke's theorem, Poincaré, Hölder and Young inequalities (for detail see Caucha et al. [26]) and taking the terms $a\colon = \big(|D|\hat{J}\|\hat{F}^{-T}\|_{\hat{\mathcal{L}}^\infty} - (\alpha_b + |\gamma h^{-2}\mathcal{H}|)\big)$ and $b\colon = \big(C(\alpha_b, c_b) + |\gamma h^{-2}\mathcal{H}c_{ext}|\big)$ and $\theta = \big(-\lambda\frac{a}{\hat{J}} + \|\hat{F}^{-1}\|_{\hat{\mathcal{L}}^\infty}\|\mathrm{div}(\partial_t\hat{T})\|_{\hat{\mathcal{L}}^\infty}\big)$ and $\hbar = \frac{b^2}{\hat{J}a}$, we have that

$$\|\hat{C}_m\|^2_{\hat{\mathcal{L}}^2} \leq \|\hat{C}_m(0)\|exp(-\theta t) + \frac{\hbar}{\theta}.$$

We see that $\hat{C}_m$ is uniform limited in $\hat{\mathcal{L}}^\infty(0, T; \hat{\mathcal{L}}^2(\hat{\Omega}))$, as it is not depend of m and t, then we say that

$$\hat{C}_m \overset{*}{\rightharpoonup} \hat{C} \quad \text{in } \hat{\mathcal{L}}^\infty(0, T; \hat{\mathcal{L}}^2(\hat{\Omega})). \tag{23}$$

Now, integrating the inequality

$$\frac{1}{2}\hat{J}\partial_t\|\hat{C}_m\|^2 - \lambda\frac{a}{2}\|\hat{\nabla}\hat{C}_m\|^2 + \frac{1}{2}\hat{J}\|\hat{F}^{-1}\|_{\hat{\mathcal{L}}^\infty}\|\hat{C}_m\|^2_{\hat{\mathcal{L}}^2}\|\mathrm{div}(\partial_t\hat{T})\|_{\hat{\mathcal{L}}^\infty} \leq \frac{b^2}{2a}$$

from 0 to T, we have

$$\int_0^T \|\hat{\nabla}\hat{C}_m\|^2_{\hat{\mathcal{L}}^2}\, dt \leq \frac{2}{|\lambda a|}\left[\hat{J}\|\hat{C}_m(0)\|^2_{\hat{\mathcal{L}}^2} + \frac{b^2}{2a}T\right]$$

then, $\hat{C}_m$ is limited in $\hat{\mathcal{L}}^2(0, T; \mathcal{H}^1(\hat{\Omega}))$, for each T, then

$$\hat{C}_m \rightharpoonup \hat{C} \ \text{ in } \ \hat{\mathcal{L}}^2(0, T; \mathcal{H}^1(\hat{\Omega})). \tag{24}$$

4. Finite Element discretization and pressure stabilization

We use Q_1 equal-order elements for velocity, pressure and gas concentration on a triangulation Ω_h. As the discrete *inf-sup* condition is violated, we have to add certain stability terms to guarantee the well- posedness of the fluid equations. we use the *Local Projection Stabilization* method (LPS) by Becker & Braack [12]. The first approach has been studied in detail for flow problems on anisotropic domains [27]. We introduce the stabilization terms on the moving domains $\Omega(t)$ first and transform the terms to the reference frame taking care of the anisotropies. Assuming that the reference grid consists of Cartesian quadrilaterals T with edge sizes $\hat{h}_x$ and $\hat{h}_y$. The cells might be arbitrarily anisotropic, however. We remark that this assumption is not necessary in general, but serves only to simplify the derivation of the stabilization.
We assume that the mesh Ω_h has a patch-hierarchy in the sense, that always four adjacent quads arise from refinement of one common patch element. We denote the mesh of patch elements by Ω_{2h}.

4.1. Local Projection Stabilization

On a Cartesian mesh, the *Local Projection Stabilization* method adds the stabilization term

$$S_{\mathrm{LPS}}(p_h, \xi_h) = \alpha_{\mathrm{LPS}} \sum_{P \in \Omega_{2h}} (h_x^2 \kappa_h \partial_x p_h, \kappa_h \partial_x \xi_h)_P + (h_y^2 \kappa_h \partial_y p_h, \kappa_h \partial_y \xi_h)_P$$

to the divergence equation. Here, we use the projection operator $\kappa_h = \mathrm{id} - i_{2h}$ and i_{2h} denotes the linear interpolation from Ω_h to Ω_{2h} (cf. [27]). For the case of more general meshes, the stabilization term might be defined in terms of two coordinate directions η_1, η_2

$$S^c_{\mathrm{LPS}}(p_h, \xi_h) = \alpha_{\mathrm{LPS}} \sum_{P \in \Omega_{2h}} \sum_{i=1}^{2} (h_i^2 \kappa_h \partial_{\eta_i} p_h, \kappa_h \partial_{\eta_i} \xi_h)_P,$$

where $\partial_{\eta_i} = \eta_i \cdot \nabla$ denotes the directional derivative and h_i is the cell size in direction η_i.
We make use of this formulation by setting

$$\tilde{\eta}_1 := \hat{F} \begin{pmatrix} \hat{h}_1 \\ 0 \end{pmatrix}, \quad \tilde{\eta}_2 := \hat{F} \begin{pmatrix} 0 \\ \hat{h}_2 \end{pmatrix}, \quad \eta_i = \frac{\tilde{\eta}_i}{\|\tilde{\eta}_i\|} = \frac{\tilde{\eta}_i}{h_i}.$$

where $\hat{h}_i$ is the length in horizontal and vertical direction of the Cartesian grid on the reference domain. Note that F and thus η_i are in general not constant within a cell and that the resulting vectors η_1, η_2 are only orthogonal in the case that the ALE map is a translation or rotation. As long as the ALE map does not degenerate, the two vectors will be linearly independent, such that stability in any coordinate direction is ensured. With these definitions, it holds that

$$h_1 \partial_{\eta_1} p_h = h_1 \eta_1 \cdot \nabla p_h = \hat{F} \begin{pmatrix} \hat{h}_1 \\ 0 \end{pmatrix} \cdot \hat{F}^{-T} \hat{\nabla} \hat{p}_h = \hat{h}_1 \hat{\partial}_1 \hat{p}_h.$$

By the same argumentation, we can show $h_2\partial_{\eta_2}p_h = \hat{h}_1\hat{\partial}_1\hat{p}_h$ as well as the same results for the test functions ξ_h. Altogether, this yields

$$\begin{aligned} S_{\mathrm{LPS}}(p_h,\xi_h) &= \alpha_{\mathrm{LPS}} \sum_{P\in\Omega_{2h}} \sum_{i=1}^{2} (h_i^2\kappa_h\partial_{\eta_i}p_h, \kappa_h\partial_{\eta_i}\xi_h)_P \\ &= \alpha_{\mathrm{LPS}} \sum_{P\in\Omega_{2h}} \sum_{i=1}^{2} \left(\hat{J}\hat{h}_i^2\kappa_h\hat{\partial}_i\hat{p}_h, \kappa_h\hat{\partial}_i\hat{\xi}_h\right)_{\hat{P}}, \end{aligned}$$

where the determinant $\hat{J}$ appears due to integral transformation. As this stabilization is equivalent to the LPS stabilization technique proposed by Braack & Richter [27] for anisotropic grids, stability and convergence estimates follow immediately from their result on the current system.
All our calculations will be done using the finite element library *Gascoigne 3d* [13]. For time discretization, we use the backward Euler time-stepping with $\delta t = 0.1$.

5. Numerical results

Considering the alveolar sac in the last generations (23rd generation), the parameters are: $D = 17\,mm^2/s$ [1, 16], $\alpha = 0.057\,ml\,CO_2/(100\,ml\,blood\,mmHg)$ CO_2 solubility in the blood [28], $c_{bl} = 0.06$ equilibrium of the CO_2 concentration in the blood [29] and $c_{\mathrm{ext}} = 0.04302$ (average of CO_2 concentration in the 22 generation at the end of exhalation).
We describe the following horizontal domain movement and keep the movement in the y-component constant.

$$x(t) = T_1(\hat{x}) = \hat{x}(1 - 0.09\cos(0.4\pi t)), \quad y(t) = \hat{y}.$$

This means that the domain at time $t = 0$ is compressed by 9% compared to the reference domain. At time $t = 2.5s$, the domain is maximally stressed and is by a factor of 1.09 bigger compared to the reference domain. The movement is periodic with period $t = 5s$.
The figure 2 shows the two different flow in the alveolar sac when the wall $\partial\Omega$ is moving, for a normal and forced maneuver. This movement makes that the pressure changed and as a consequence permit that the gas flow enter by Γ_{io}.

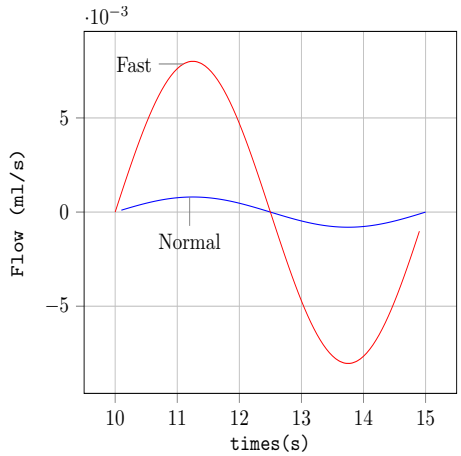

Figure 2 - Different flow rate for a normal and forced maneuver.

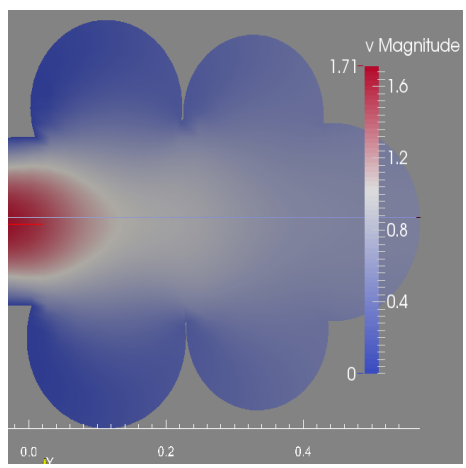

Figure 3 - Inflow for a normal maneuver.

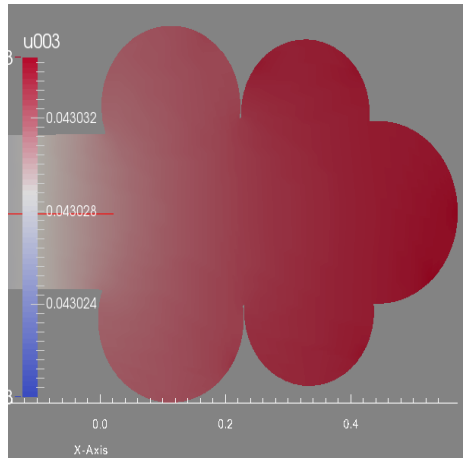

Figure 4 - CO_2 concentrations for a normal maneuver.

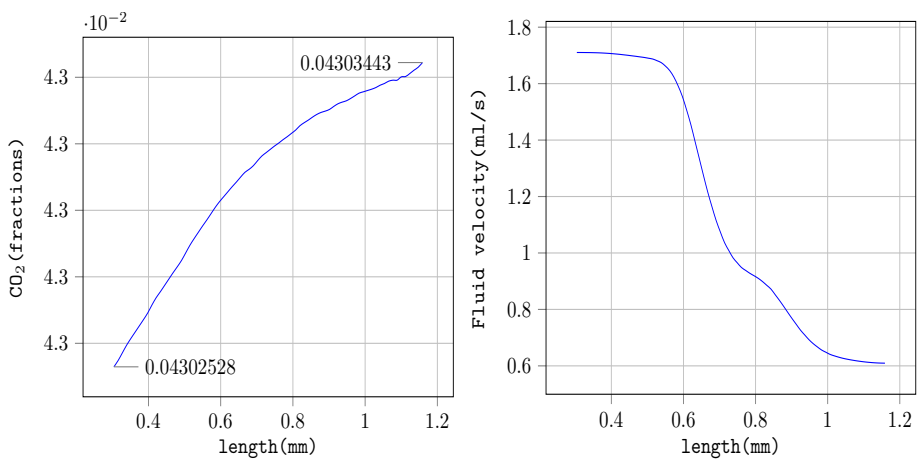

Figure 5 -CO_2 concentration and flow rate in the alveolar sac (normal maneuver).

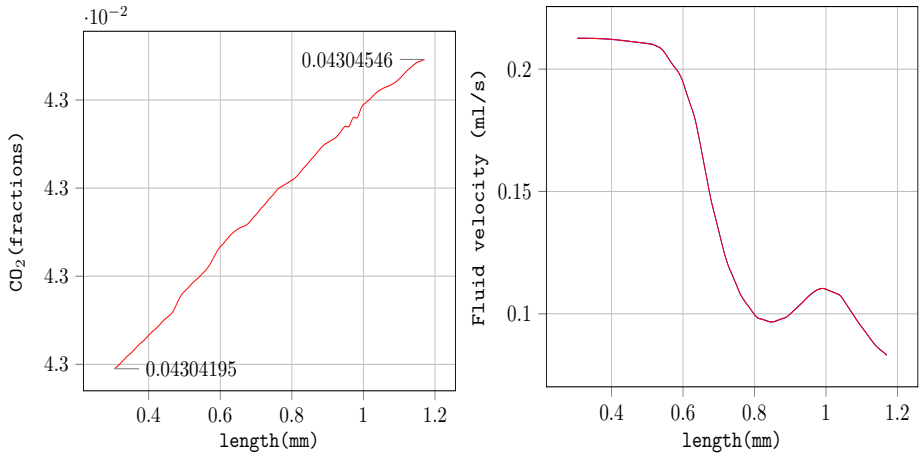

Figure 6 -CO_2 concentration and flow rate in the alveolar sac (fast maneuver).

The figure 3 shows the distributions for inflow in the alveolar sac at $t = 1.25s$. Those curves were taken in line straight down the middle in the alveolar sac.
In the figure 4 show the gas transportation from the blood to the alveolar sac, we can see the dilution of carbon dioxide as a consequence of the gas inhaled.
Making the curve in line straight down the middle in the alveolar sac for the CO_2 concentrations, we can see the carbon dioxide stratification, that curve changes depending of the maneuver, see on right side in the figures (5 and 6). Those values increase as a consequence of the gas exchange with blood CO_2 concentration of 0.065;

6. Conclusion

The analysis of weak solution for the model of the dynamics of gases exchange in Arbitrary Lagrangian-Eulerian coordinate showed that the dissipation of energy for the fluid that transports of gases is a function of the properties of fluid and the velocity of domain deformation of the alveolar sac. Furthermore, the dissipation for the concentration of carbon dioxide, it does not depend on fluid velocity as a consequence of incompressible fluid; the finite element method with equal-order element and local projection stabilization permitted to simulated the change of CO_2 concentrations in the alveolar sac, it will help to study the dynamic of gas in different part of the lungs.

Future work: Analysis of dynamics of gases considering fluid-structure interaction, and analysis of dynamics in lung pathologies.

Acknowledgments. This work was supported by PNICP-Perú, N 361 $-$ $PNICP - PIBA -$ 2014.

References

[1] Scherer, P. W., Shendalman, L. H., Green, N. M., Simultaneous diffusion and convection in single breath lung washout, Bull. Math Biophys 34: 393-412, 1972.

[2] Weibel, E. R., Morphometry of the human lung, Berlin:Springer, 1963.

[3] Paiva, M., Engel, L., Model Analysis of intra-acinar gas exchange, Respiration Physiology 62: 257-272, 1985.

[4] Engel, L., Gas mixing within the acinus of the lung, J. Appl. Physiol. 54:609-618, 1983.

[5] Felici, M., Filoche, M., Sapoval, B., Diffusional screening in the human pulmonary acinus, J. Appl. Physiol. 94: 2010-2016, 2003.

[6] Scrimshire, D. A., Tomlin, P. J., Ethridge, R. A., Computer simulation of gas exchange in human lungs, J. Appl. Physiol. 34(5): 687-696, 1973.

[7] Swan, A. J., Tawhai, M. H., Evidence for minimal oxygen heterogeneity in the healthy human pulmonary acinus, J. Appl. Physiol. 110: 528-537, 2011.

[8] Federspiel, W. J., Fredberg, J. J., Axial dispersion in respiratory bronchioles and alveolar ducts, J. Appl. Physiol. 64(6): 2614-2621, 1988.

[9] Hughes, T. J. R., Liu, W. K., Zimmermann, T., Lagrangian-Eulerian finite element formulation for incompressible viscous flows, Comput. Methods Appl. Mech. Engrg. 29:329-349, 1981.

[10] Donéa, J., Fasoli-Stella, P., Giuliani, S., Lagrangian and Eulerian finite element techniques for transient fluid-structure interaction problems, Structural mechanics in reactor technology, 1977.

[11] Wall, Wolfgang A., Rabczuk, T., Fluid–structure interaction in lower airways of CT-based lung geometries, International Journal for Numerical Methods in Fluids 57(5):653-675, 2008.

[12] Becker, R., Braack, M.,: A finite element pressure gradient stabilization for the Stokes equations based on local projections, Calcolo 38(4): 173-199, 2001.

[13] Becker, R., Braack, M., Meidner, D., Richter, T., Vexler, B., The finite element toolkit Gascoigne 3d, http://www.gascoigne.uni-hd.de.

[14] Cruz, J.C.,Jeng, D-R., Han, D., Wu, G., Flores, X. F., Ventilation inhomogeenties and mixed venous blood N2 in multibreath N_2 Washout, Respir. Physiol. 110: 47-56, 1997.

[15] Cruz, J. C., A Combined parallel and series distribution model of inspired inert gases, Respir. Physiol. 86: 1-14, 1991.

[16] Scherer, P. W., Gobran, S., Aukburg, S. J., Baumgardner, J. E., Bartkowski, R., Neufeld, G. R., Numerical and experimental study of steady-state CO_2 and inert gas washout, J. Appl. Physiol. 64(3): 1022-1029, 1988.

[17] Caucha, L. J., Sanchez, R. A., Arredondo, R. N., Mathematical simulation of the gases transport (O_2 and CO_2) in the alveolar zone of the human lung for normal breath and force maneuver, Revista Manglar 10(2): 39-48, 2013.

[18] Braack, M., Mucha, P. B., Directional do-nothing condition for the Navier-Stokes Equations, Journal of Computational Mathematics 35(5): 507-521, 2014.

[19] Becker, R., Mesh adaptation for Dirichlet flow control via Nitsche's method, Commun. Numer. Meth. Engng. 18:669-680, 2002.

[20] Dunne, T., Adaptive Finite Element Approximation of Fluid-Structure Interaction Based on Eulerian and Arbitrary Lagrangian-Eulerian Variational Formulations, University of Heidelberg, 2007.

[21] Dziri, R., Zolesio, J. P., Eulerian derivative fof non-cylindrical functionals, Shape optimization and optimal design 216:87-108, 2001.

[22] author =Grandmont, C., Existence for a Three-Dimensional Steady State Fluid-Structure Interaction Problem, J. Math. fluid mech. 4:76-94, 2002.

[23] Galdi, G. P., Rannacher, R., Fundamental Trends in Fluid Structure Interaction, World Scientific Publishing Co., 2010.

[24] Du, Q., Gunzburger, M. D., Hou, L. S., Lee, J., Analysis of a linear fluid-structure interaction problem, Discrete and continuous dynamical systems 9(3):633-650, 2003.

[25] Temam, R., Navier-Stokes Equation and Nonlinear Functional Analysis, CBMS-NSF Regional Conference Series in Applied Mathematics (SIAM, Philadelphia),66,1995.

[26] Caucha, L. J., Rubio, O., Rodriguez, A., Existence and uniqueness of solutions to a model for dynamic of CO_2 in the alveolar sac of the human lung, Submitted to NonLinearity, 2016.

[27] Braack, M., Richter, T., Local projection stabilization for the Stokes system on anisotropic quadrilateral meshes, Numerical Mathematics and Advanced Applications, 770-778, 2006.

[28] Suresh, V., Anderson, J. C., Grotberg, J. B., A Mathematical Model of Alveolar Gas Exchange in Partial Liquid Ventilation, J. Bio. Eng. 127: 46-59, 2005.

[29] West, J. B., Regional differences in gas exchange in the human lung of erect man, J. Appl. Physiol. 17:893-898, 1962.